Exploring the Effects of Blank Holding Force and Friction Coefficient Variations on Aluminum Alloy Deep Drawing: A Finite Element Analysis

[1]Om Prakash Vishwakarma, [2]Mr.Pankaj Pandey, [3]Girish Kumar Khare

[1]Mtech Scholar, Department of Mechanical Engineering, Oriental Institute of Science & Technology, Bhopal India,

[2]Assistant Professor, Department of Mechanical Engineering, Oriental Institute of Science & Technology, Bhopal India.

[3]Associate Professor, Mechanical Engineering Oriental Institute of Science & Technology, Bhopal India.

[1]omprakashvishwakarma98@gmail.com, [2]pankajpandey@oriental.ac.in, [3]oisthodme@oriental.ac.in

* Corresponding Author: Mr. Pankaj Pandey

Abstract: *In deep drawing operation the sheet metal deformation can occurs due to the relative movement between the punch tool and the sheet, an interaction that generates friction forces occurred between the elements. The main objective of the present work is to analyze the effect of punch displacement, stresses produced in blank during the cup drawing operation with the variation in parameter blank holding force and friction coefficient for different aluminum alloy using finite element analysis. For that two different aluminium alloys (AA1050 & AA1100) have been used with three different frictional coefficients such as 0.005, 0.01 & 0.02. The blank holding force for the cylindrical deep drawing has been calculated using mathematical relation. The result show that as the friction force increased the contact pressure force also increased, in the present work minimum contact pressure force occurs for AA1050 material. Since the minimum stress is produced for the same materials, for the better results of cylindrical deep drawing AA1050 can be used.*

Keywords: *Finite element analysis, aluminum alloys, contact pressure, cylindrical deep drawing, spring-back, optimization*

I.INTRODUCTION

Deep drawing, a prominent forming procedure, involves the transformation of sheet metals by pressing them into a die cavity to achieve desired shapes. This intricate operation relies on the application of tensile and compressive forces onto a metal blank, facilitated by a combination of mechanical action and mold configuration shows in figure 1. Its versatility and efficiency have rendered deep drawing a cornerstone in various industrial sectors, contributing to the production of items ranging from soda cans to kitchen tools and electrical instruments [1].In the realm of process optimization and material science, accounting for the strain rate dependency of materials has emerged as a crucial consideration in deep drawing design. Models such as the Johnson-Cook approach, Cowper-Symonds, and others have been instrumental in capturing this nuanced behavior, where the yield stress is influenced by the rate at which deformation occurs. While traditionally, the strain rate sensitivity of materials was often overlooked in numerical simulations at room temperature, recent insights suggest its significance, particularly in scenarios where forming velocities exceed standard material characterization rates [3,5].

High-speed forming tests, conducted at elevated strain rates, have shed light on the profound impact of strain rate sensitivity, even at room temperature, especially concerning the prediction of crash behavior [6]. This realization prompts a fundamental question: can incorporating strain rate dependency into material models enhance the accuracy of numerical simulations, not only in high-speed applications but also in scenarios with lower stamping velocities? Moreover, considering the spatial and temporal variations in strain rates during the deep drawing process, there arises an additional consideration for localized strain rate dependent modeling, potentially applicable even in processes with fixed stamping velocities.In this context, this paper explores the implications of strain rate sensitivity in deep drawing processes, aiming to elucidate its role in enhancing prediction quality and process optimization. By bridging theoretical insights with practical implications, this study seeks to contribute to the advancement of deep drawing methodologies and their applications across diverse industrial domains.

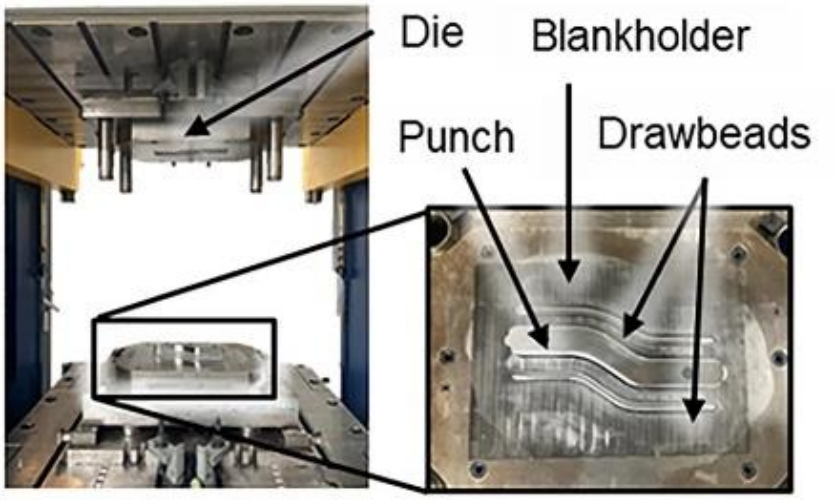

Figure.1 Experimental setup for the deep drawing process [4].

A. Understanding the Basics of Cup Production of Deep Drawing Process

Different types of disposable cups were commonly used nowadays such as plastic cups, paper cups, and styro cups due to their convenience. However, these said products which are known for being single-use only usually end up as waste and increase the rate of pollution. The most effective biodegradable alternative for these disposable cups is polylactic acid also known as corn plastic but this product still has downfall for the most part of the following: The duration of composting for industrial composter is not acquired; The residue is not ability of the soil or in short, there is no nutrient added; And lastly, it increases the pH value of the soil resulting in an increase in acidity. By making a plant based biodegradable cup made from different means to trash materials, namely wood scobs, bamboo sawdust, and coconut husk, a potential solution can be created to the increasing amount of non-biodegradable waste mainly in disposable cups. As shows in figure 2. reusable cup manufacturing which describe by flow chart in which manufacturing of reusable cup in different stages of power system, detergent manufacture etc. By reducing prospective non-biodegradable waste, there is a possibility of decreasing the level of global warming, climate change, and production of micro plastics. Glass cups, although common in households, are very inconvenient to use compared to other types of cups.

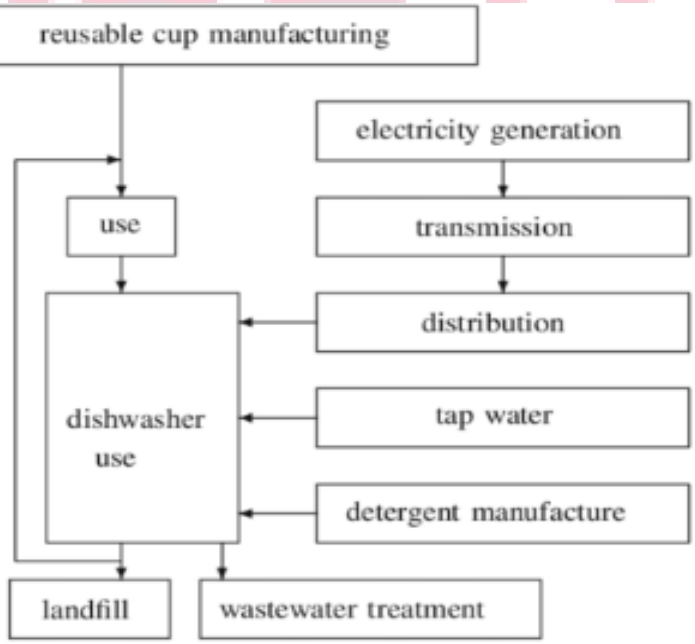

Figure. 2 Reusable cup manufacturing [13].

B.The Significance of Deep Drawing in Cup Manufacturing

The deep drawing process holds immense significance within the realm of cup manufacturing, spanning two comprehensive pages of discussion. At its core, deep drawing epitomizes efficiency and precision, offering a pathway to

crafting cups endowed with uniformity and finesse. This metal forming technique entails the meticulous transformation of flat metal sheets into three-dimensional structures, executed through the strategic application of pressure and tensile forces. In the realm of cup production, this method emerges as a cornerstone, facilitating the seamless creation of vessels boasting smooth contours and consistent thickness. A schematic of the conventional deep drawing process for sheet metal is shown in Fig. 3. It is to be note that film free side of the laminate is in contact with the punch during deep drawing. The deep drawing for all different laminated specimens (A, B, C and metallic films) were performed on a MTS mechanical testing machine fitted with two servo-controlled actuators as shown in Figure 3.

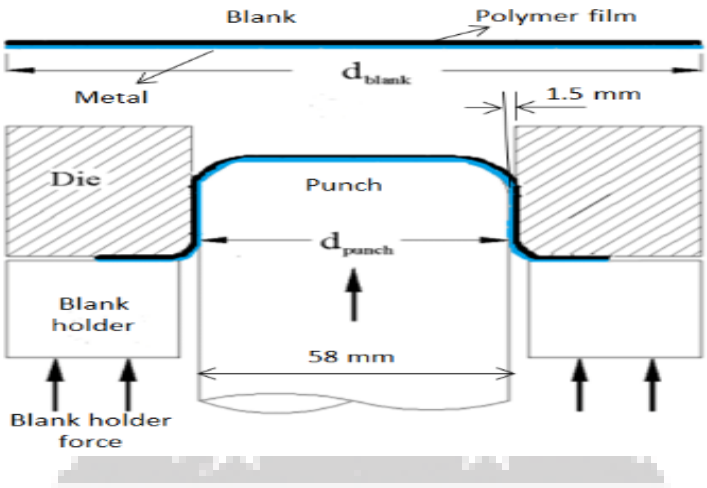

Figure 3. A schematic of cup deep drawing process [17]

Moreover, the versatility of deep drawing extends beyond the realms of shape and size, encompassing an extensive array of materials. Whether it be stainless steel, aluminum, or various plastics, the deep drawing process readily accommodates the unique properties of each substrate. This flexibility not only fosters innovation in design but also enhances the functional attributes of the final product. Cups fashioned through deep drawing exhibit a remarkable degree of robustness and durability, rendering them suitable for a myriad of applications across diverse industries

II. LITERATURE REVIEW

Mrabti et al. (2023) conducted a comprehensive investigation into the deep drawing process, focusing on the significance of various parameters such as die section radius, blank holder force, and friction coefficients. Their study employed finite element modeling in ABAQUS, validated with experimental results, and utilized Taguchi design and analysis of variance (ANOVA) methods to identify critical parameters affecting the square-drawing process.

Mohsein et al. (2023) aimed to optimize deep drawing processes for producing pentagonal cups, comparing two distinct methods through numerical simulations and experimental tests. Using ANSYS 20 software, they evaluated the impact of drawing methods on load distribution, stress/strain patterns, and thickness uniformity, concluding that the choice of forming method significantly influences the final product's characteristics.

Luyen et al. (2023) focused on selecting an appropriate yield criterion to accurately describe the anisotropic behavior of materials in deep drawing processes. Through finite element simulations and experimental validation using SPCC material, they compared von Mises, Hill'48R, and Hill'48S yield functions, emphasizing the crucial role of the chosen yield criterion in predicting fracture height accurately

Another study by Luyen et al. (2023) investigated the effect of elevated temperatures on the deep drawing of cylindrical cups using SPCC sheet steel. Through numerical simulations and experimental validations, they optimized process parameters such as blank holder force and punch radius to achieve uniform thickness distribution, providing valuable insights for improving deep drawing processes.

Sundar Singh Sivam et al. (2023) developed a multistage micro-deep drawing technology to manufacture microcups, focusing on parameters like tool force, spring back, and forming limit curve. Their study integrated finite element analysis (FEA) with real-time trials to optimize process parameters and ensure high-quality microstructures in the final products.

III. OBJECTIVE

- To minimize the stress produced during the deep drawn cup at all regions.
- To optimized punch displacement and punch pressure for different design of aluminums alloy sheet material.
- To minimize spring-back effect occurs in the drawn component with the help of equivalent plastic strain in FEM analysis.

IV. METHODOLOGY

Deep drawing operation depends on various parameters such as Blankholder Pressure, Clearance between Punch and Die, Corner Radius of Punch and Die, Lubrication etc.

A. Base Model geometry of cylindrical cup drawing

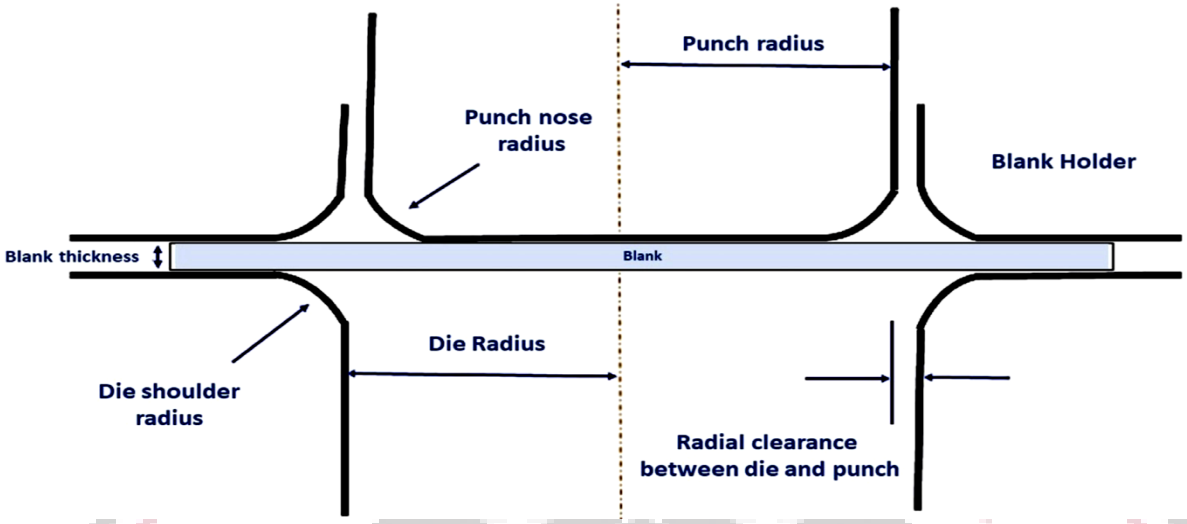

Figure 4. Base Model geometry of cylindrical cup drawing

The table 1.outlines the dimensions, measured in millimeters, of key parameters relevant to the tooling employed in the cylindrical cup drawing process. These parameters include the Punch Radius (30 mm), Punch Nose radius (6 mm), Blank Size radius (51 mm), Blank thickness size (1.5 mm), Blank holder radius (65 mm), Die radius (31.5 mm), and Die shoulder radius (5 mm). These dimensions play a critical role in shaping the final product, affecting factors such as the outer shape, inner surface smoothness, thickness, and overall quality of the formed cylindrical cups.

Table 1. Tool dimensions for cylindrical cup drawing

Parameters	Dimensions in mm
Punch Radius	30
Punch Nose radius	6
Blank Size radius	51
Blank thickness size	1.5
Blank holder radius	65
Die radius	31.5
Die shoulder radius	5

B.SOLID186 Element Description

SOLID186 is a higher order 3-D 20-node solid element that exhibits quadratic displacement behavior. The element is defined by 20 nodes having three degrees of freedom per node: translations in the nodal x, y, and z directions. The element supports plasticity, hyperelasticity, creep, stress stiffening, large deflection, and large strain capabilities. It also has mixed formulation capability for simulating deformations of nearly incompressible elastoplastic materials, and fully incompressible hyperelastic materials that also Shows in figure 5.

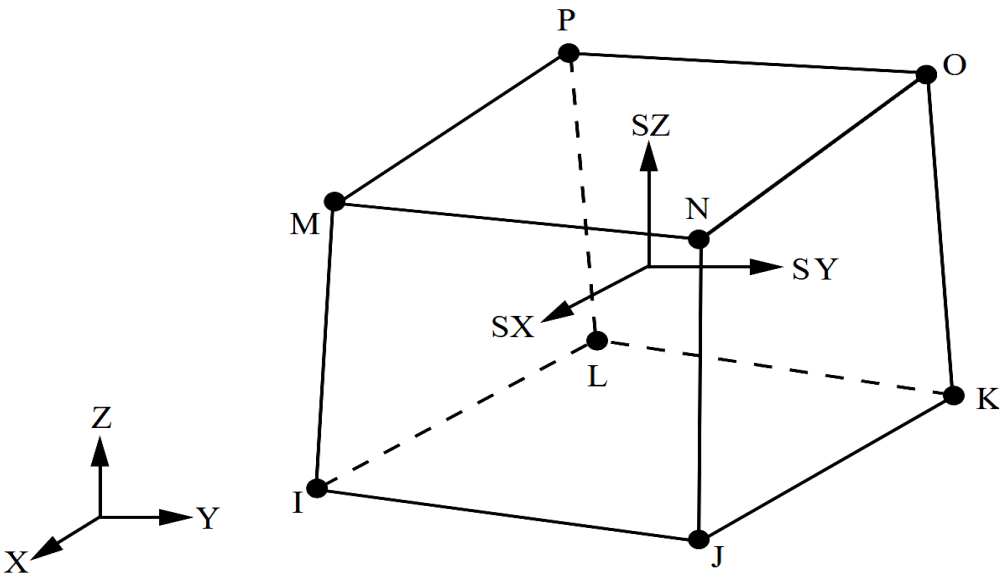

Figure 5. SOLID185 3-D structural solid (ANSYS manual)

C.CONTA174 Geometry

CONTA174 is used to represent contact and sliding between 3-D target surfaces and a deformable surface defined by this element. The element is applicable to 3-D structural and coupled-field contact analyses. It can be used for both pair-based contact and general contact Shows in figure 6.

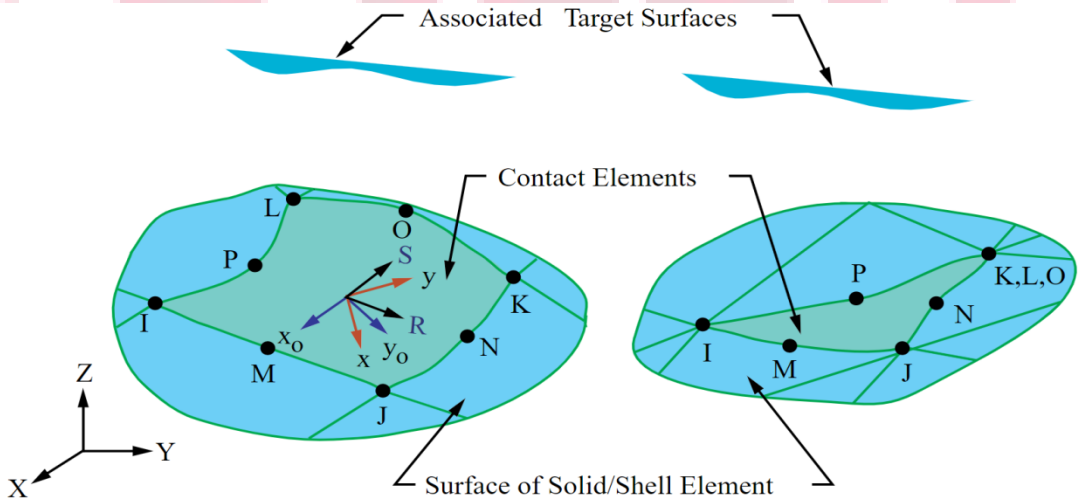

Figure 6. CONTA174 (ANSYS manual)

D.TARGE170 Element Description

TARGE170 is used to represent various 3-D "target" surfaces for the associated contact elements (CONTA173, CONTA174, CONTA175, CONTA176 and CONTA177). The contact elements themselves overlay the solid, shell, or line elements describing the boundary of a deformable body and are potentially in contact with the target surface, defined by TARGE170.

a) Assumptions Made in the Simulations

- The material is assumed to be isotropic which means that it has similar properties in all directions.
- The mechanical interaction between the contact surfaces is assumed to be the frictional contact.

E.CAD model

The three dimensional axisymetry CAD model of cylindrical cup drawing is developed using key-point methods in ansys mechanical apdl. The Punch Radius 30 mm, Punch Nose radius is 6 mm, Blank Size radius is 51 mm, Die radius is 31.5 mm Die shoulder radius is 65 mm with Blank thickness size as 1 mm as shown in figure 7.

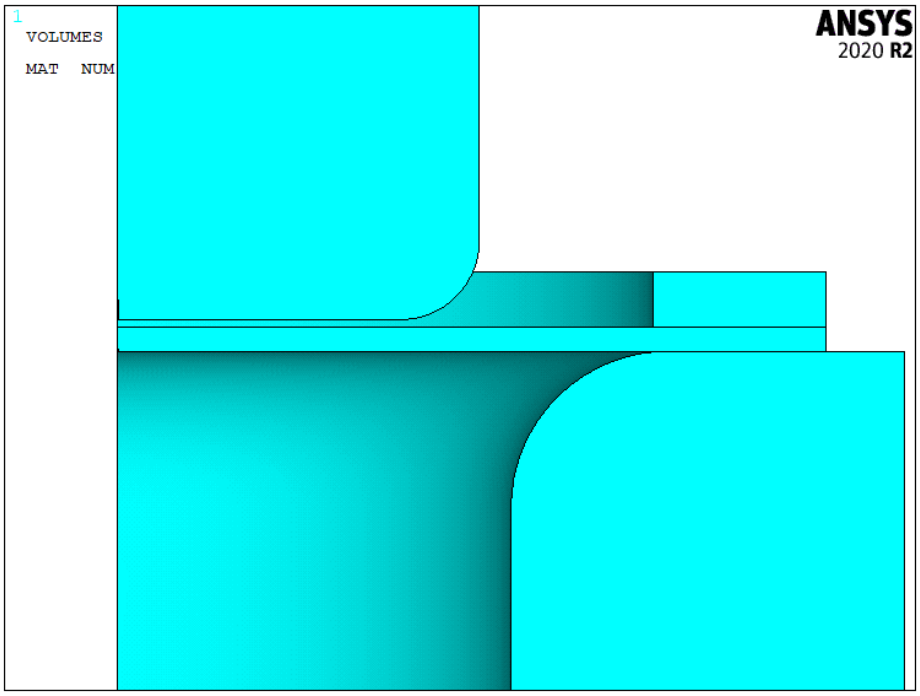

Figure 7 (a): Front view of CAD modeling for cylindrical cup drawing

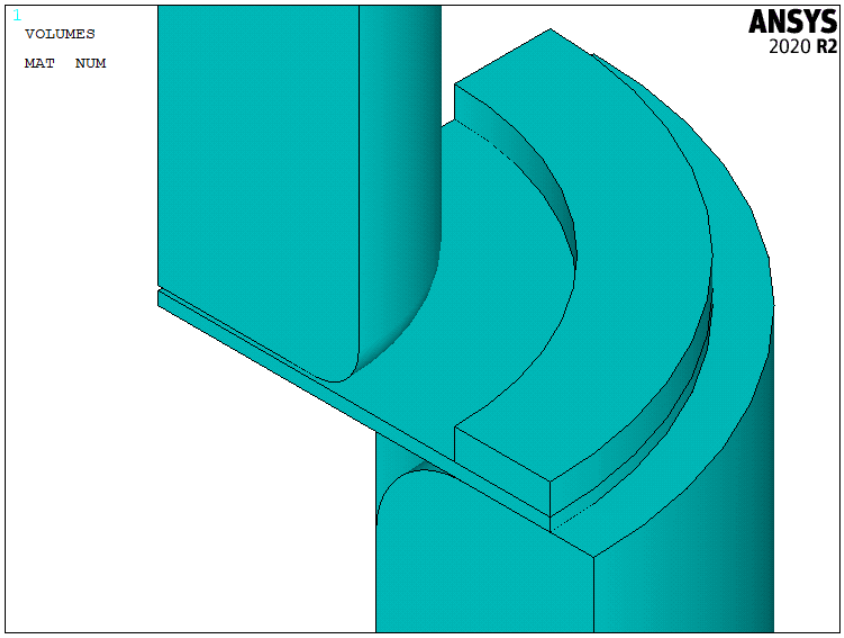

Figure 7 (b): Isometric view of CAD modeling for cylindrical cup drawing

Meshing is a critical operation in finite element analysis in this process CAD geometry is divided into large numbers of small pieces called mesh, total no of nodes generated in the present work is 11856 and total no. of elements is 13155. Quadrilateral elements have been created as shown in figure 8.

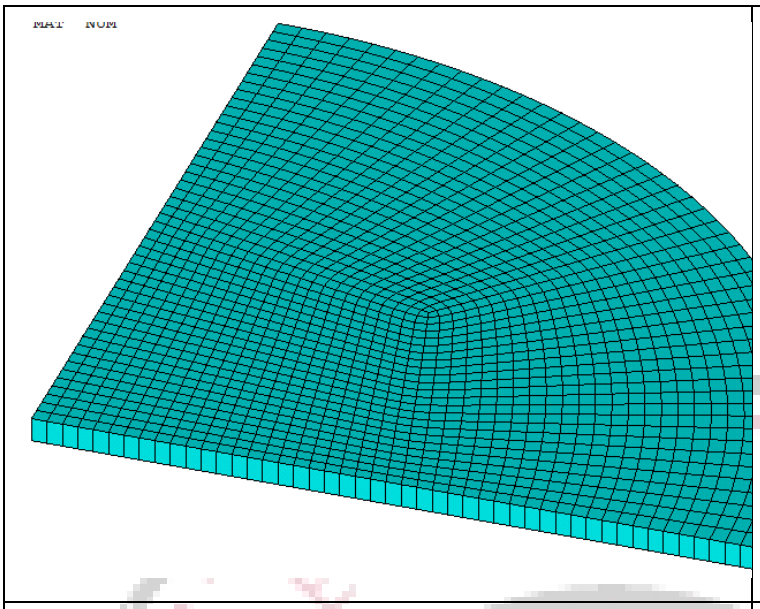

Figure 8. (a): Meshing of un-deform blank for cylindrical cup drawing

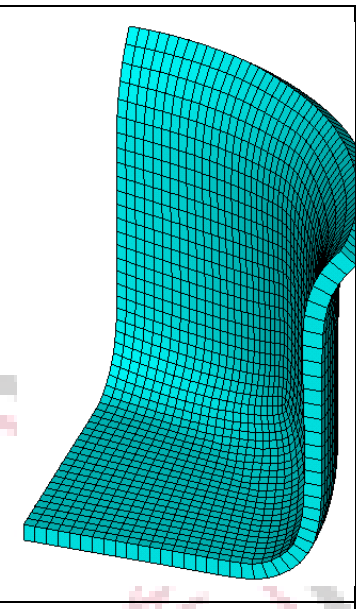

Figure 8. (b): Meshing of deform blank for cylindrical cup drawing

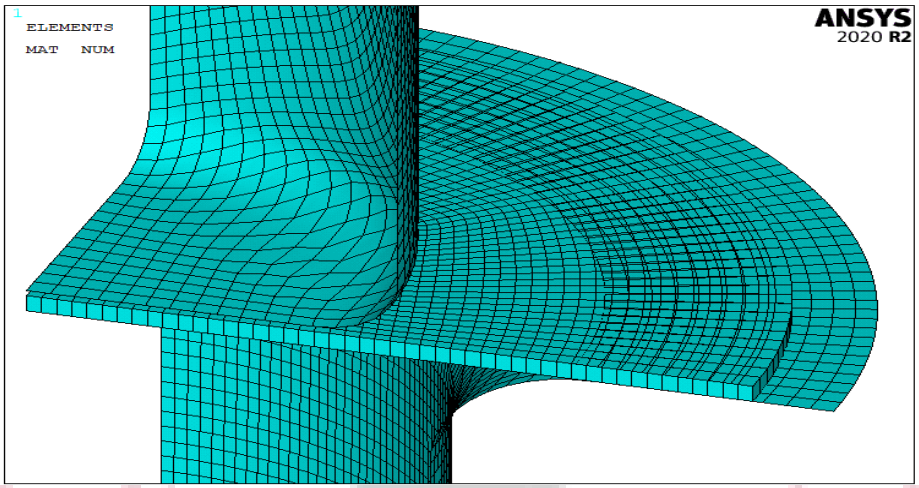

Figure 8. (c): Meshing of complete assembly of for cylindrical cup drawing

Table 2. showsAA1050 and AA1100 alloys exhibit notable differences in their material properties. AA1050 has a slightly higher density of 2700 kg/m3 compared to AA1100's 2710 kg/m3. However, AA1050 boasts a higher tensile strength coefficient (k) of 149 MPa, along with a significantly greater strain hardening exponent (n) of 0.287, indicating enhanced resistance to plastic deformation compared to AA1100's 0.019. Both alloys have comparable yield stress values, with AA1050 at 68.9 MPa and AA1100 at 69 MPa. AA1050 shows higher plastic anisotropy across all orientations (r_0, r_45, r_90) than AA1100. Additionally, their hardening laws differ significantly: AA1050's hardening law follows 149(0.0035+ε)^0.287, while AA1100's is expressed as 47.9+99*ε^0.19. These distinctions highlight the importance of selecting the appropriate alloy based on specific mechanical and performance requirements in engineering applications.

Table 2. Material properties for the AA1050 and AA1100

Material	**AA1050**	**AA1100**
Density (Kg/m3)	2700	2710
Tensile Strength coefficient (k) MPa	149	99

Strain hardening exponent (n)	0.287	0.019
Yield stress (MPa)	68.9	69
ε_0	0.0035	-
Poissons ratio	0.33	0.33
r_0	0.8	0.649
r_{45}	0.55	0.667
r_{90}	0.89	0.611
Hardening laws	$149(0.0035+\varepsilon)^{0.287}$	$47.9+99*\varepsilon^{0.19}$

V.RESULT ANALYSIS

The Comparative results of cylindrical cup drawing for AA1050 & AA1100 shows in table 3.Provides data for different scenarios in cylindrical cup drawing, including Blank Holder Force (BHF) in MPa, friction coefficient (μ), displacement, maximum and minimum Von-Mises stress, equivalent plastic strain, and contact pressure.

Table 3. Comparative results of cylindrical cup drawing for AA1050 & AA1100

S. no.	BHF (MPa)	μ	Displacement	Von-mises stress		Eq. Plastic strain		Contact Pressure
				Max	Min	Max	Min	
1	16855	0.005	35.5355	239.18	20.0104	0.6045	0.03035	181.861
2	16855	0.01	32.7472	239.18	33.7215	0.5696	0.03035	175.304
3	16855	0.02	30.7886	239.18	32.2369	0.5358	0.03035	220.299
4	16879	0.005	33.6414	239.18	25.4646	0.5849	0.03035	156.026
5	16879	0.01	31.572	239.18	32.4806	0.5519	0.03035	162.902
6	16879	0.02	30.2663	239.18	33.6245	0.5269	0.03035	274.662

From the above result analysis it has been observed that the maximum displacement for punch of 35.5355 mm for AA1050 at 0.005 friction coefficient while the minimum displacement of 30.2663 mm for AA1100 at 0.02 friction coefficient.

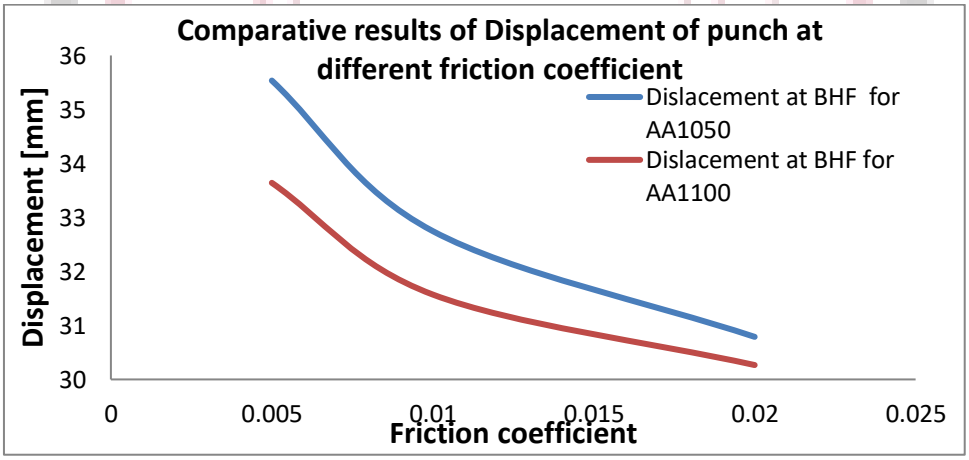

Figure 9. Comparative results of Displacement of punch at different friction coefficient

Figure 9 shows Comparative results of Displacement of punch at different friction coefficient displacement of punch for AA1050 and AA1100.

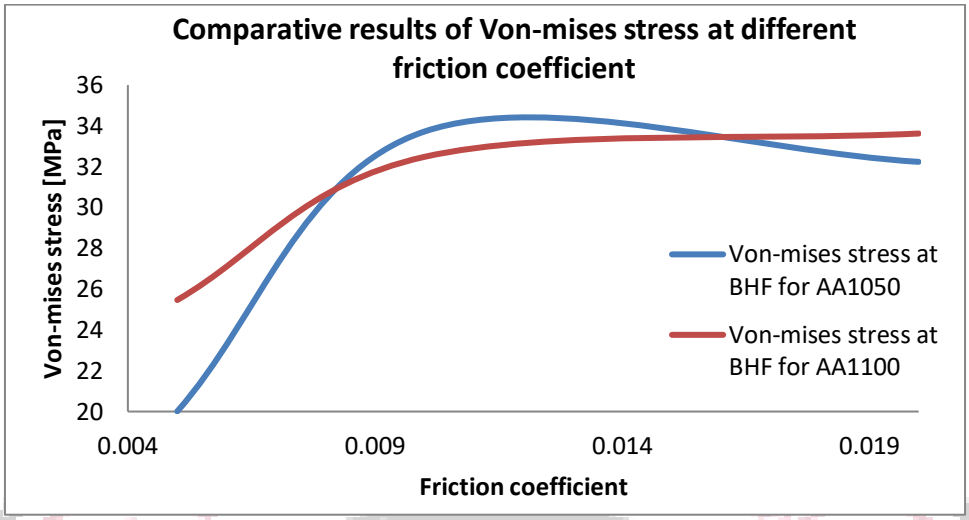

Figure 10. Comparative results of Von-mises stress at different friction coefficient

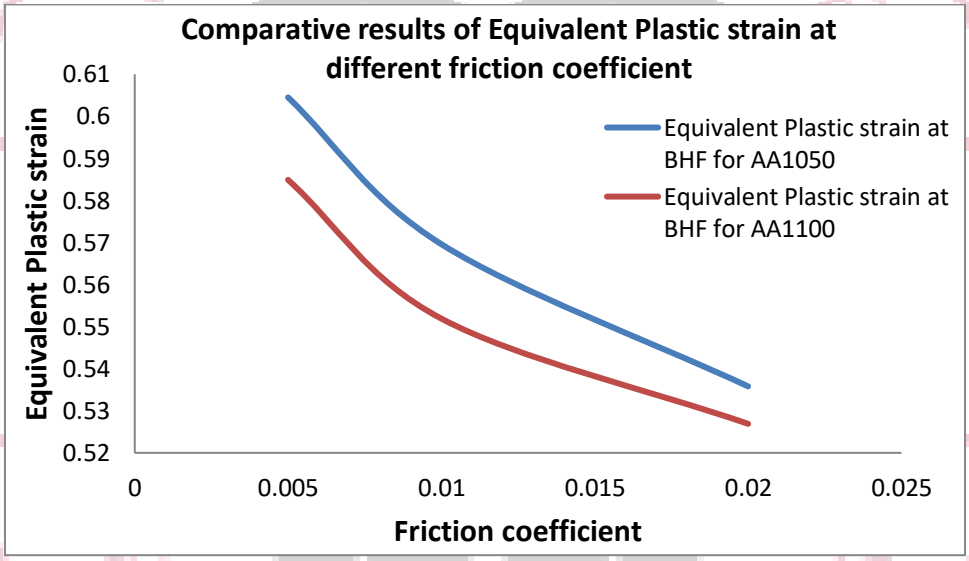

Figure 11.Comparative results of Equivalent Plastic strain at different friction coefficient

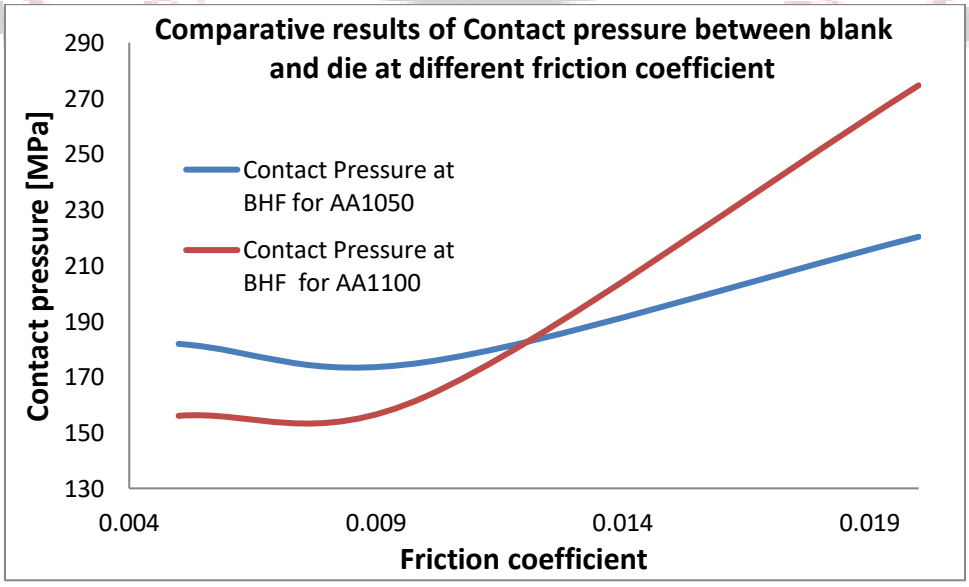

Figure 12. Comparative results of Contact pressure between blank and die at different friction coefficient

The Von Mises stresses are mainly used for ductile material where design fails when the induced stress in the material is greater than the strength of the material. The maximum von-Miss stress obtained in this present work is 239.18 MPa. Equivalent plastic strain is a measure of the permanent strain in a structure. This plastic strain is mapped from the partially plastic strain identified in the equivalent strain domain. The maximum contact pressure between blank and die is 274.662 for AA1100 at 0.02 friction coefficient show in table 12.

Table 4. Comparative results of principle stress of cylindrical cup drawing for AA1050 & AA1100

S. no.	BHF (MPa)	μ	1st Principal stress		2nd Principal stress		3rd Principal stress	
			Max	Min	Max	Min	Max	Min
1	16855	0.005	161.982	-0.1824	75.6592	-78.34	24.9687	-242.143
2	16855	0.01	168.775	0.8347	88.2466	-70.2894	22.5755	-240.46
3	16855	0.02	184.252	1.1641	101.547	-74.0384	20.1187	-239.399
4	16879	0.005	159.386	0.5616	79.5883	-77.8916	24.0226	-241.458
5	16879	0.01	178.13	1.7616	96.7658	-74.2734	20.7973	-239.903
6	16879	0.02	191.692	1.5332	106.031	-79.3186	19.1424	-240.072

From the above result in table 4.analysis it has been observed that the first principal stress gives the estimation of stress that is normal to the planewhere the shear stress is zero, the maximum value of 1st principal stress in the present work is 191.692 MPa for AA1100 at 0.02 friction coefficients. The third principal stress that is normal tothe plane where the shear stress is zero, the maximum value of 3rd principal stress in the present work is 24.9687 MPa for AA1050 at 0.005 friction coefficients.

V.CONCLUSION

In conclusion, the analysis conducted in this study aimed to investigate the effects of punch displacement, stresses induced in the blank, and variations in blank holding force and friction coefficient on the cup drawing operation for different aluminum alloys through finite element analysis. The results revealed distinct behaviors for AA1050 and AA1100 alloys across different frictional coefficients, with varying levels of displacement, stresses, contact pressures, and equivalent plastic strains observed. Particularly, it was noted that increasing friction force led to higher contact pressure, with AA1050 exhibiting lower contact pressures and stresses compared to AA1100. Therefore, for optimal cylindrical deep drawing outcomes, AA1050 may be preferred. In terms of future work, expanding the study to include additional materials and exploring more frictional parameters could offer further insights into the deep drawing process.

REFERENCES

[1] Tiwari, P. R., Rathore, A., &Bodkhe, M. G. (2022). Factors affecting the deep drawing process–A review. Materials Today: Proceedings, 56, 2902-2908.

[2] Zerilli, F. J., & Armstrong, R. W. (1987). Dislocation-mechanics-based constitutive relations for material dynamics calculations. Journal of applied physics, 61(5), 1816-1825.

[3] Doege, E., Meyer-Nolkemper, H., & Saeed, I. (1986). FließkurvenatlasmetallischerWerkstoffe: mitFließkurvenfür 73 Werkstoffe und einergrundlegendenEinführung. Hanser.

[4] Vallaster, E., Wiesenmayer, S., &Merklein, M. (2024). Effect of a strain rate dependent material modeling of a steel on the prediction accuracy of a numerical deep drawing process. Production Engineering, 18(1), 47-60.

[5] Tekkaya AE, Pöhlandt K, Dannemann E (1982) MethodenzurBestimmung der Fließkurven von Blechwerkstoffen. EinÜberblick: Teil II. BlechRohre Profile 354–359.

[6] Larour, P., Bäumer, A., Dahmen, K., &Bleck, W. (2013). Influence of strain rate, temperature, plastic strain, and microstructure on the strain rate sensitivity of automotive sheet steels. steel research international, 84(5), 426-442.

[7] Trattnig, G., Lind, C., Sommitsch, C., Feuerhuber, H., &Winklhofer, J. (2010, June). Process Simulation of Aluminium Sheet Metal Deep Drawing at Elevated Temperatures. In 10th International Conference on Numerical Methods in Industrial Forming Processes.

[8] Tulke, M., Galiev, E., Psyk, V., Kräusel, V., &Brosius, A. (2022, May). Deep drawing of DC06 at high strain rates. In IOP Conference Series: Materials Science and Engineering (Vol. 1238, No. 1, p. 012047). IOP Publishing.

[9] Psyk, V., Scheffler, C., Tulke, M., Winter, S., Guilleaume, C., &Brosius, A. (2020). Determination of material and failure characteristics for high-speed forming via high-speed testing and inverse numerical simulation. Journal of Manufacturing and Materials Processing, 4(2), 31.

[10] Vallaster, E., Wiesenmayer, S., &Merklein, M. (2024). Effect of a strain rate dependent material modeling of a steel on the prediction accuracy of a numerical deep drawing process. Production Engineering, 18(1), 47-60.

[11] Menezes, L. F., &Teodosiu, C. (2000). Three-dimensional numerical simulation of the deep-drawing process using solid finite elements. Journal of materials processing technology, 97(1-3), 100-106.

[12] Guia, Jardy&Bancifra, Christene& Leon, Elijah & Perez, Leah & Reyes, Frank &Lanuang, Milbert. (2024). Utilization of plant-based biodegradable cup as alternative to disposable cup. International Journal of Science and Research Archive. 11. 1030-1041. 10.30574/ijsra.2024.11.2.0535.

[13] Merugula, Laura &Bakshi, Bhavik. (2014). Reusable vs. disposable cups revisited: Guidance in life cycle comparisons addressing scenario, model, and parameter uncertainties for the US consumer. The International Journal of Life Cycle Assessment. 19. 931-940. 10.1007/s11367-013-0697-7.

[14] Liewald, M., Bergs, T., Groche, P., Behrens, B. A., Briesenick, D., Müller, M., ...& Müller, F. (2022). Perspectives on data-driven models and its potentials in metal forming and blanking technologies. Production Engineering, 16(5), 607-625.